[19]W. L. Hafner, Jr., J. R. Huizenga, and R. Vandenbosch, Argonne National Laboratory Report No. ANL-6662, 1962 (unpublished).
[20]G. A. Bartholomew *et al.*, Nucl. Data A3, 367 (1967).
[21]H. W. Newson and J. H. Gibbons, in *Fast Neutron Physics*, edited by J. B. Marion and J. L. Fowler (Interscience, New York, 1963), Pt. II, p. 1601.
[22]D. Sperber and J. W. Mandler, Nucl. Phys. A113, 689 (1968).

PHYSICAL REVIEW C VOLUME 6, NUMBER 2 AUGUST 1972

Reaction-Mechanism Study in the $1f$-$2p$ Shell of (^{16}O,^{12}C) Four-Nucleon-Transfer Reaction

P. Bonche and B. Giraud
Service de Physique Théorique, Centre d'Etudes Nucléaires de Saclay, France

and

A. Cunsolo,* M.-C. Lemaire, M. C. Mermaz, and J.-L. Québert†
Service de Physique Nucléaire à Basse Energie, Centre d'Etudes Nucléaires de Saclay, France
(Received 27 March 1972)

The (^{16}O,^{12}C) four-nucleon-transfer reaction has been performed on a ^{54}Fe target using the 46-MeV ^{16}O beam of the FN tandem Van de Graaff at Saclay. The study of the reaction ^{54}Fe-(^{16}O,^{12}C)^{58}Ni shows that the four-nucleon transfer occurs via a direct surface reaction, well described by the quasielastic process formalism due to Frahn and Venter, which is based on the diffractional model. The transfer-reaction cross sections are peaked at the grazing angle where the elastic scattering begins to deviate from the pure Rutherford law. A distorted-wave Born-approximation investigation of nuclear properties of levels reached by (^{16}O,^{12}C) four-nucleon transfer has been performed using the SETILL code based on the generator-coordinate framework. The Q-value dependence of the cross section, as well as the configuration mixing effects, has been estimated. The cases of other $1f$-$2p$-shell nuclei have been also investigated.

I. INTRODUCTION

It is well known that (^{7}Li, t) and (^{16}O, ^{12}C) reactions have provided relevant spectroscopic information about four-nucleon transfer in the $2s$-$1d$ shell and $2p$-$1f$ shell, respectively. Qualitative analysis of the α-like structure observed in the Ca and Ni regions with the (^{16}O, ^{12}C) reaction have been extensively reported in terms of the quartet model.[1] It had already been shown that quartetting phenomena[2] as predicted by V. Gillet play a very important role in the nuclear structure of the $1f$-$2p$ shell, mainly in the vicinity of doubly magic $N=Z$ nuclei such as ^{40}Ca and ^{56}Ni. The purpose of this paper is to investigate the (^{16}O, ^{12}C) four-nucleon-transfer mechanism above the Coulomb barrier and to present a preliminary distorted-wave Born-approximation (DWBA) analysis for α-like transfer induced by heavy ions.

The nature of the reaction mechanism can be qualitatively understood in terms of the Frahn and Venter quasielastic formalism built on the framework of the diffractional model.[3] Nevertheless, we may feel that the four-nucleon spectroscopic information can be extracted only through a complete finite-range DWBA calculation including a *microscopic-nuclear-structure form factor*. The present results seem to show that such a DWBA analysis is valid for the description of the reaction mechanism.

The (^{16}O, ^{12}C) reaction experiments have been performed on a ^{54}Fe target isotope, at 46-MeV incident energy, for which both the entrance and exit channels are above the Coulomb barrier. The angle corresponding to a *grazing collision* is then located around 60° c.m. In the discussion part of this paper, other (^{16}O, ^{12}C) transfer reactions will be considered for the $1f$-$2p$ shell.

II. EXPERIMENTAL PROCEDURE

The experiments reported here have been performed in a scattering chamber with two solid-state telescopes, using the ^{16}O beam of the Saclay FN tandem Van de Graaff. The thickness of each of the first silicon surface-barrier ΔE counters was 10 μm. The identification of the detected heavy fragments was carried on line using the fol-

lowing identification function $F(Z) = \Delta E + 0.16E$. The $F(Z)$ summation was performed in the analogic part of our electronic setup described in Ref. 1. The empirical value of 0.16 is in agreement with the heavy-ion range measurements of Northcliffe's data[4] for a 10-μm-thick Al screen. The separation is well achieved between the various isotopes such as O, N, and C, but not so well between different masses for a given charge Z. Nevertheless, in the ^{54}Fe target case, among the various C isotope channels, only the ^{12}C one is allowed, since the Q values of the other ones are far too negative.

The target used was 100 μg/cm^2 thick and made of 99% enriched ^{54}Fe isotope on a 20-μg/cm^2 carbon backing. The ^{16}O beam intensity was 400 nA for an average charge state of 7.5. A self-supporting Fe target would not resist so strong an ^{16}O-ion flux.

Figure 1 presents a typical spectrum of the (^{16}O, ^{12}C) reaction obtained at 42.5° and 46-MeV ^{16}O incident energy. The resolution is 225 keV, mainly due to target thickness, kinematic broadening, and kinematic shift.

III. ABSOLUTE CROSS-SECTION DETERMINATION

The ^{16}O elastic cross section has been measured at 46-MeV incident energy between 15 and 90° lab angle and obeys the Rutherford scattering law up to 55° c.m. angle. The ratios between elastic scattering yield and (^{16}O, ^{12}C) α transfer yield have been measured at forward angles and are directly proportional to the ratios of the corresponding cross sections in the laboratory system. From the Rutherford absolute cross section we have then deduced the (^{16}O, ^{12}C) transfer-reaction cross-section value.

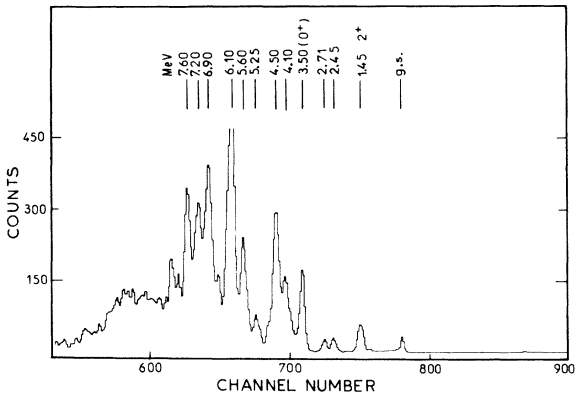

FIG. 1. ^{12}C spectrum obtained from the reaction ^{54}Fe-(^{16}O, ^{12}C)^{58}Ni at 46-MeV ^{16}O incident energy and at 42.5° lab angle. The energy resolution is 225 keV.

IV. EXPERIMENTAL RESULTS WITH DIFFRACTIONAL MODEL ANALYSIS

A. Elastic Scattering

The oxygen elastic angular distributions have been measured at three different energies, 46, 48, and 52 MeV, in 5° steps between 15° lab and for some of them, up to 100° lab. As it can be seen in Fig. 2, the cross sections obey, respectively, the Rutherford scattering law up to 55, 50, and 45° c.m. After a rise above the Rutherford cross-section limit, the intensities decrease monotonically and exponentially at backward angles. This

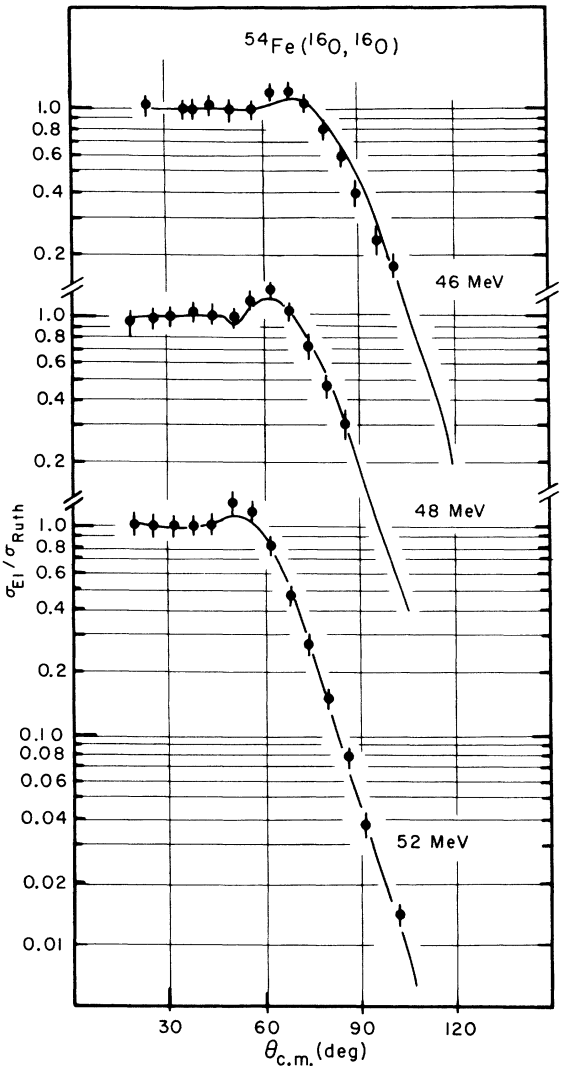

FIG. 2. Experimental elastic scattering angular distributions measured, respectively, at 46-, 48-, and 52-MeV ^{16}O incident energy. The fits were obtained using the smooth cutoff diffractional model on the Frahn and Venter parametrization (see Table I).

behavior without any oscillatory structure is the signature of diffraction scattering of the Fresnel type due to strong absorption phenomena in presence of a high Coulomb barrier[5]; and it is not surprising, since the ratio η/k is much larger than 1. The quantity $\eta = Z_1 Z_2 e^2/\hbar v$ is the Sommerfeld parameter and k the incoming wave number.

The elastic scattering has been studied within the framework of the diffractional model using the parametrization of Frahn and Venter to define the smooth-cutoff approximation.[6]

The total scattering amplitude is written in the usual way,

$$f(\theta) = f_C(\theta) + \frac{i}{2k} \sum_{l=0}^{\infty} (2l+1)(1-\eta_l) e^{2i\sigma_l} P_l(\cos\theta) , \tag{4.1}$$

and the cross section is expressed by

$$\sigma(\theta) = |f(\theta)|^2 ,$$

where $f_C(\theta)$ is the asymptotic Coulomb part of the scattering amplitude, σ_l the Coulomb phase shift, and η_l the nuclear phase shift.

In the Frahn and Venter semiclassical parametrization, the reflection coefficients η_l are given by the following Woods-Saxon forms:

$$\mathrm{Re}\eta_l = (1 + e^{(L_c - l)/\Delta})^{-1} , \tag{4.2}$$

$$\mathrm{Im}\eta_l = \frac{\mu}{\Delta} e^{(L_c - l)/\Delta} (1 + e^{(L_c - l)/\Delta})^{-2} .$$

Here the critical angular momentum L_c is given by

$$L_c = kR(1 - 2\eta/kR)^{1/2} + \tfrac{1}{2} , \tag{4.3}$$

and the diffuseness parameter Δ in angular momentum space is related to the diffuseness parameter d in ordinary space by the following formula:

$$\Delta = kd(1 - \eta/kR)(1 - 2\eta/kR)^{-1/2} . \tag{4.4}$$

The nuclear radius is chosen to be

$$R = r_0(A_1^{1/3} + A_2^{1/3}) .$$

The elastic scattering fit depends then only on three parameters, r_0, $\mu/4\Delta$, and d.

In Table I are listed the values of these parameters corresponding to the 46-, 48-, and 52-MeV best elastic scattering fits displayed in Fig. 2. Only the radius $r_0 = 1.55$ fm, which is obtained from the Blair[7] "one-quarter-point recipe," is well determined. Otherwise, there is an ambiguity for d and $\mu/4\Delta$, which are both responsible for the slope of the backward elastic cross sections. We shall see later on that the diffuseness parameter d is partially determined in a quasi-elastic process such as a cluster-transfer reactions.

The elastic angular distributions have been also analyzed with the Saclay optical-model code MAGALI of Raynal.[8] In the presence of strong absorption phenomena, it is only the tail of the optical-potential well which can be determined, and we have used Woods-Saxon forms for the real and imaginary parts, both having the same geometry.

All the elastic fits are of exactly the same quality as those presented in Fig. 2 and obtained with the diffraction phase-shift analysis. The optical-model parameters corresponding to the best 46-MeV elastic scattering fits for various real well depths (V_0) are listed in Table II. The logarithms of $V_0 e^{R/a}$ and of $W_0 e^{R/a}$, shown in the two last columns, are remarkably constant. This feature confirms that it is only the tails of the potential that have been determined, as expected in a heavy-ion scattering analysis. This was pointed out many years ago by Igo and Thaler[9] for α elastic scattering.

TABLE I. Phase-shift-analysis parameter (see text); r_0 is given by the "one-quarter-point recipe" (Ref. 7) and is the only well-defined parameter; d is the diffuseness parameter of the potential well.

$E_{^{16}O}$ (MeV)	r_0 (fm)	d (fm)	$\mu/4\Delta$
46	1.55	0.325	0.284
48	1.55	0.320	0.500
52	1.55	0.45	0.310

TABLE II. Optical-model parameters obtained with the MAGALI code of Raynal (Ref. 8) corresponding to ^{16}O elastic scattering on ^{54}Fe target measured at 46-MeV incident energy. χ^2 is the best-fit parameter, $\ln V + R/a$ and $\ln W + R/a$ reported in the two last columns indicate that it is only the remote tails of the Woods-Saxon well potential which have been determined as expected in presence of strong absorption phenomena:

$$V(r) = V_{\mathrm{Coul}}(R) + (V_0 + iW_0)(1 + e^{(R-r)/a})^{-1} ,$$

$$R = r_0(54^{1/3} + 16^{1/3}) ,$$

$$\chi^2 = \frac{1}{N} \sum_{i=1}^{N} \left(\frac{\sigma^i_{\mathrm{exp}} - \sigma^i_{\mathrm{opt}}}{\Delta\sigma^i_{\mathrm{exp}}} \right)^2 .$$

V_0	W_0	r_0	a	χ^2	$\ln V + R/a$	$\ln W + R/a$
100	18.81	1.154	0.55	0.58	17.82	16.15
200	35.09	1.094	0.55	0.56	17.82	16.09
300	51.56	1.059	0.55	0.55	17.82	16.06
400	67.67	1.034	0.55	0.55	17.82	16.04
500	84.23	1.014	0.55	0.55	17.82	16.04
600	100.30	0.998	0.55	0.55	17.82	16.03
700	115.19	0.985	0.55	0.55	17.83	16.03

B. (^{16}O, ^{12}C) Four-Nucleon-Transfer Reaction

The (^{16}O, ^{12}C) angular distributions of all the ^{58}Ni excited states displayed in Fig. 1 have been measured between 30 and 75° lab angle. They all exhibit the same shape and are peaked around 60° c.m., corresponding to the grazing angle at 46-MeV incident energy. At this angle, the elastic angular distribution begins to deviate from the pure Rutherford scattering law (see Fig. 2).

The general behavior of this reaction angular distribution can be explained with very simple semiclassical considerations. The transfer cross section reaches its maximum value at the grazing distance (or the so-called apsidal distance), where the impact parameter $D+(\eta/k)(1+1/\sin\frac{1}{2}\theta)$ is equal to the sum of the heavy-fragment interaction radii. At backward angles, the cross sections decrease exponentially owing to the competition with strong absorption phenomena. At forward angles, where the impact parameter is larger than the sum of the nuclear radii of two fragments, the transfer process occurs only through the interaction in the tail region of the transferred cluster.

A parametrization of this transfer process is given by the Frahn and Venter formalism.[3] The real part of the η_l reflection coefficients as mentioned previously is given by a Woods-Saxon form (see Fig. 3). Then it is natural to consider that the direct-transfer amplitudes, as well as any kind of direct inelastic process, are proportional to the derivative of the η_l reflection coefficient amplitude (lower curve of Fig. 3).

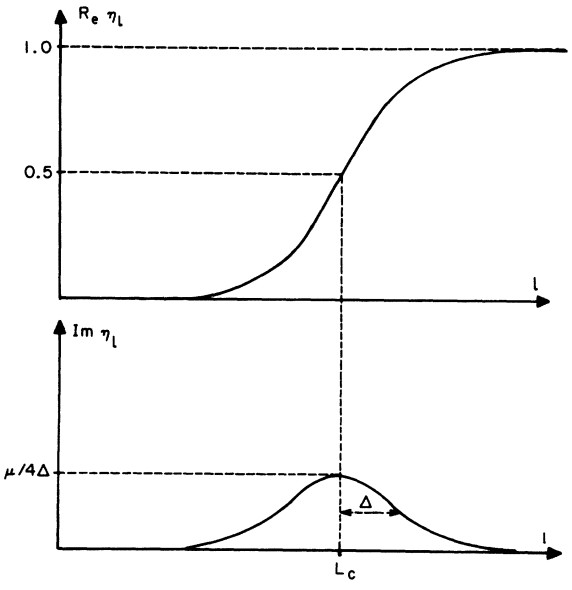

FIG. 3. Qualitative form of the real and imaginary parts of reflection coefficient function η_l in the Frahn and Venter parametrization.

The transfer amplitude can be then written as

$$f_T(\theta)=\frac{i}{2k}\sum_{l=0}^{\infty}(2l+1)e^{2i\sigma_l}\eta_l' P_l(\cos\theta)\,, \tag{4.5}$$

where

$$\eta_l'=\tau\frac{\partial}{\partial l}(1+e^{(L_c-l)/\Delta})^{-1}\,, \tag{4.6}$$

with the same notation as defined previously and with τ being the phenomenological spectroscopic amplitude of the transfer reaction.

From the above expression Frahn and Venter have been able to derive for the cross section the following analytical formula:

$$\frac{d\sigma}{d\Omega}=\tau^2\frac{L_c}{2k^2\sin\theta}[F_+^{\,2}+F_-^{\,2}+2F_-F_+\sin(2L_c\theta)]\,, \tag{4.7}$$

where

$$F_\pm(\theta)=\frac{\pi\Delta(\theta\pm\theta_c)}{\sinh[\pi\Delta(\theta\pm\theta_c)]}\,,$$

θ_c being the grazing angle

$$\theta_c=2\arctan(\eta/L_c)\,. \tag{4.8}$$

A better fit for the over-all set of angular distribution is achieved by arithmetically averaging the k, η, and R parameters of the incoming and outgoing channels. This procedure allows us to reproduce the gradual shift of the grazing angle θ_c observed in cluster-transfer reactions as the excitation energy of the final state increases. Figures 4 and 5 summarize the results, the fits are in rather good agreement with the experimental data. The τ constant values, given in Table III, are taken as normalization constants of the experimental points with respect to the calculated curves. The quantity labeled $\tau/4\Delta$ is simply the maximum value of $\eta_l'=\eta_{L_c}'$ as seen from Eq. (4.6), and the maximum of the transfer-reaction amplitude is directly proportional to this phenomenological quantity. The two other free parameters, for all the fits, are the radius $r_0=1.90$ fm, which fixes the calculated position θ_c, and the diffuseness parameter $d=0.375$ fm, which is responsible for the angular width of the differential cross section. Herein, the r_0 value corresponds to the grazing angle θ_c and not the much more backward one corresponding to the "one-quarter-point recipe"[7] in the elastic scattering phase-shift analysis.

A very important effect which is completely neglected in the Frahn and Venter quasielastic formalism is the experimentally observed Q-value dependence of the cross-section magnitude. This effect can be qualitatively understood, as pointed

TABLE III. Semiclassical parameters of the cluster-transfer cross section given by the Frahn and Venter quasielastic process analysis. θ_c is the grazing angle, L_c is the critical angular momentum of the diffractional model for which nuclear scattering amplitude is $\frac{1}{2}$, Δ is the diffuseness parameter in the angular momentum space, τ is the phenomenological spectroscopic amplitude of the cluster-transfer reaction, and $\tau/4\Delta$ is the maximum reaction amplitude at the nuclear surface for $l=L_c$.

Exc. (MeV)	θ_c (deg)	L_c	Δ	τ^2	$\tau/4\Delta$
g.s.	58	30.3	0.483	0.017	0.07
1.45	59.7	29.4	0.487	0.06	0.12
2.46; 2.77	61	28.8	0.491	0.045	0.11
3.52	62.6	28.1	0.495	0.16	0.20
4.10	63	27.7	0.496	0.22	0.24
4.50	64.1	27.5	0.498	0.36	0.30
5.60	66	26.7	0.502	0.24	0.25
6.10	66.9	26.4	0.504	0.79	0.43
6.90	68.4	25.8	0.508	0.59	0.38
7.20	69.3	25.6	0.509	0.37	0.30
7.60	69.8	25.3	0.510	0.47	0.23

out by Von Oertzen,[10] following the Buttle and Goldfarb arguments.[11] The DWBA transition matrix elements reach their maximum values when the incoming and outgoing wave functions present a maximum overlap. With the optical wave function being dominated by the Coulomb field, this occurs semiclassically when the apsidal distances in the entrance and exit channels are equal:

$$\frac{z_i Z_i}{2E_{\text{c.m.}}}\left[1+1/\sin\left(\tfrac{1}{2}\theta_i\right)\right]=\frac{z_f Z_f}{2(E_{\text{c.m.}}+Q)}\left[1+1/\sin\left(\tfrac{1}{2}\theta_f\right)\right]. \tag{4.9}$$

Neglecting the small difference between θ_i and θ_f due to the kinematics of the reaction, this expression leads to the following optimum Q-value expression for an α-like-transfer reaction:

$$Q_{\text{opt}}=-\left(1-0.75\frac{Z_i+2}{Z_i}\right)E_{\text{c.m.}}\,. \tag{4.10}$$

For an $^{54}_{26}Fe_{28}$ target at 46-MeV ^{16}O incident laboratory energy this corresponds to a Q value of -6.9 MeV, and to an excitation energy of 6.14 MeV in the ^{58}Ni residual nucleus. As can be noticed from Fig. 1, the strength of the excited groups is distributed around this 6-MeV value. However, the first levels up to 3.50 MeV are much more weakly excited for another reason: from a spectroscopical point of view, as often explained previously,[1] they correspond to two neutron states in $^{58}_{28}Ni_{30}$,[12] the 4p-2h strength starting only above 3.50-MeV excitation energy. This argument is based on the assumption that the $^{54}_{26}Fe_{28}$ target ground state can be described in a first approximation as a $(1f_{7/2})^2_{J_p=0}$ two-proton-hole state. It should also be noticed that the 3.50-MeV group is excited by the $^{56}_{26}Fe_{30}(^{16}O, ^{14}C)^{58}_{28}Ni_{30}$ two-proton transfer.[13] Moreover, a γ-^{12}C coincidence experiment had shown that in the reaction $^{54}_{26}Fe_{28}(^{16}O, ^{12}C)$-$^{58}_{28}Ni_{30}$, the level mainly populated seems to be the 3.52-MeV 0^+ level.[14] The lifetime of this state had been measured by Start *et al.*[15] with a Doppler-shift-attenuation method. The $B(E2, 0_3^+ \rightarrow 2_1^+)$ of this 3.52-MeV level is 77 $e^2\,\text{fm}^4$, which is a rather large value.

V. DWBA INVESTIGATION OF QUARTETTING PHENOMENA

A. DWBA Formalism

Although the detailed mechanism of transfer reaction between heavy ions is far from being well understood, we have admitted that a DWBA analysis might be a suitable tool to extract a complete spectroscopic information. In a four-nucleon-transfer process, it is not obvious at all that the DWBA cross section can be factorized as in the one-nucleon-transfer case, in terms of a product of two spectroscopic factors by a "single-particle" reduced cross section. The calculation has to take detailed account of the four-nucleon correlations due to angular momentum coupling and two-body interactions in the projectile and in the residual nucleus. Such correlations can be α-like, but various other types of configuration mixing are possible.

For the general understanding of our preliminary analysis, we are presenting briefly here the finite-range DWBA formalism[16] based on an application[17] on the generator-coordinate theory.[18] The transition matrix elements are written in terms of single integrals for the optical-model wave functions and on a *nuclear-structure form factor*. The form factor is an independent integral calculated with the second-quantization technique. In this calculation, recoil effects in the entrance and exit channels are taken into account in a symmetrical way. For the reaction of the type $b(A, a)B$ the transition matrix element can be written as (forgetting for the sake of simplicity spin and angular momentum coupling)

$$T_{i\to f}\propto\int \chi_f^{(-)*}\left(\frac{\mu_i}{\mu_f}\vec{X}\right)F\left(\frac{M}{M_A+M_B}\frac{M_b}{M_B}\vec{X}\right)\chi_i^{(+)}(\vec{X})\,d\vec{X}, \tag{5.1}$$

where X plays the role of a distance between the incoming ion A and the target nucleus b. The quantities μ_i and μ_f are the reduced masses in the entrance and in the exit channel. M_A, M_b, M_a, and M_B are, respectively, the masses of the projectile, the target nucleus, the outgoing particle, and

the residual nucleus. Furthermore, we have $M = M_a + M_B = M_A + M_b$.

The form factor $F(\vec{\rho})$ is expressed in the following way:

$$F(\vec{\rho}) = \int d\vec{r}_1 d\vec{r}_2 d\vec{r}_3 d\vec{r}_4 \phi_f(\vec{r}_1)\phi_f(\vec{r}_2)\phi_f(\vec{r}_3)\phi_f(\vec{r}_4) \times [U(\vec{r}_1) + U(\vec{r}_2) + U(\vec{r}_3) + U(\vec{r}_4)] \times \mathcal{A}\phi_i(\vec{r}_1 - \vec{\rho})\phi_i(\vec{r}_2 - \vec{\rho})\phi_i(\vec{r}_3 - \vec{\rho})\phi_i(\vec{r}_4 - \vec{\rho})$$

with

$$\vec{\rho} = \frac{M}{M_A + M_B}\frac{M_b}{M_B}\vec{X} \ . \tag{5.2}$$

In this expression, $\mathcal{A}$ is the antisymmetrization operator between the four transferred particles. The $\phi_{i,f}$ are the single-nucleon shell-model wave functions, correctly bound, in the projectile and in the residual nucleus. The variable $\vec{r}$ stands for the coordinates of the captured nucleons in the residual nucleus and $\vec{r} - \vec{\rho}$ stands for the coordinates of the transferred nucleons in the incoming ion.

The form factor $F(\vec{\rho})$ can be written in the alternative form

$$F(\vec{\rho}) = \langle 0 | \hat{C} U \hat{D}^\dagger(\vec{\rho}) | 0 \rangle \ . \tag{5.3}$$

The operator $\hat{C}^\dagger$ and $\hat{D}^\dagger$ create the four transferred particles in states bound, respectively, to cores b and a. The vector $\vec{\rho}$ indicates that these particles are referred, respectively, to cores b and a and should be a reminder of the fact that they are created at different places. This description presents some analogies with a two-center shell model. This last expression for $F(\vec{\rho})$ has the advantage of showing how second-quantization techniques can be used to avoid any Talmi-Moshinsky transformation, the form factor being simply a

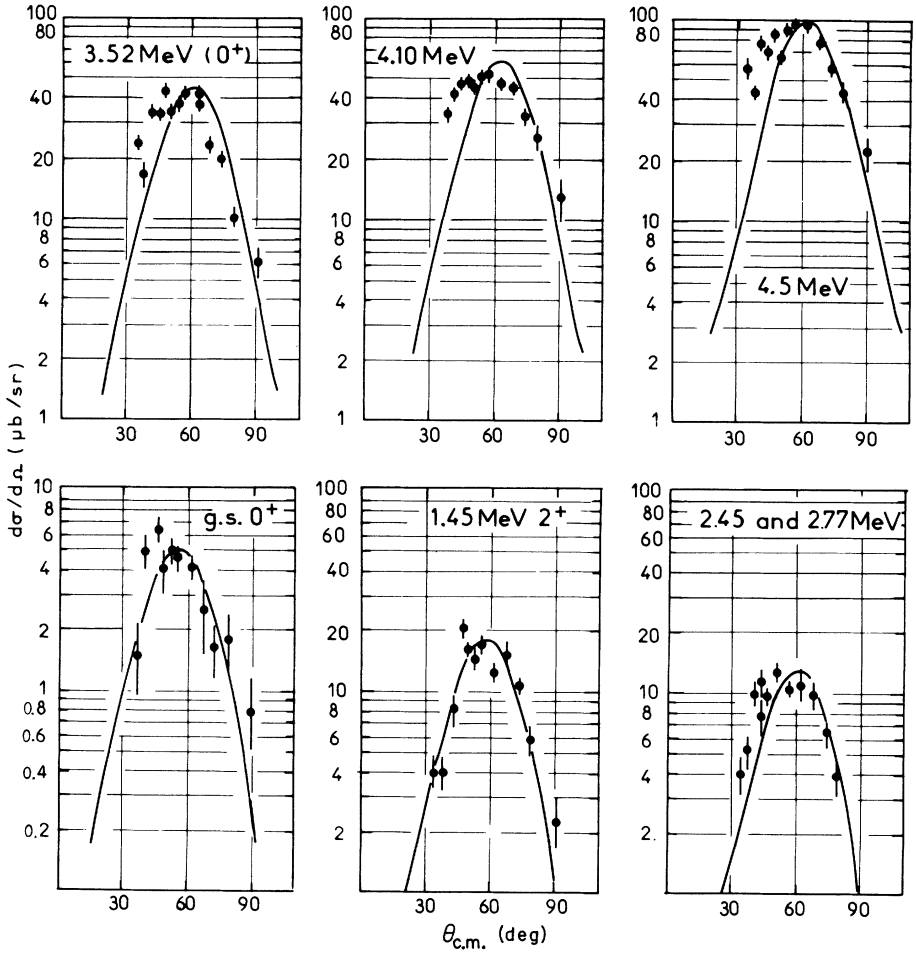

FIG. 4. Experimental $^{54}Fe(^{16}O, ^{12}C)^{58}Ni$ angular distributions measured at ^{16}O 46-MeV incident energy. The curves have been calculated with the Frahn and Venter formulas based on the general diffractional model.

product (or sum of products) of convolution integrals between single-particle wave functions.

B. Results of the DWBA Analysis

(1) Description of the projectile. In the present calculation performed with the SETILL code,[19] it has been assumed that the four nucleons in the ^{16}O projectile occupy the $1p_{1/2}$ subshell, neglecting then the possible mixing with particles in the $2s$-$1d$ shell.

(2) Influence on cross sections of configuration mixing in the residual nuclei. It turns out that one of the most striking features of the present DWBA calculations is a great sensitivity of the cross-section magnitudes to the configuration mixing in the residual states reached by the four-nucleon-transfer reaction. On the other hand, the shape of angular distributions are almost insensitive to any configuration admixture. This behavior of the cross section has been investigated using a stretch-model wave function in which each proton-neutron pair is coupled to the maximum angular momentum allowed, the two pairs being then recoupled to the final nuclear spin J_f of the residual nucleus. Figure 6 shows the cross-section intensity for different $(1f_{7/2})^4_J$ and $(2p_{3/2})^4_J$ configuration admixtures taking as an example the reaction $^{40}Ca(^{16}O, ^{12}C)^{44}Ti$ and assuming the 1.082-MeV 2^+ level has the following stretch-model wave function:

$$|Q, 2^+\rangle = a(1f_{7/2})^4_{J_f=2} \pm (1-a^2)^{1/2}(2p_{3/2})^4_{J_f=2} . \tag{5.4}$$

There is a factor of 50 in the calculated cross-section values between a transition populating the extreme $(2p_{3/2})^4$ and $(1f_{7/2})^4$ pure configuration. In the $1f$-$2p$ shell, nuclear-structure form-factor calculations show that in general $[(2p_{3/2})^{p,n}_3; (2p_{3/2})^{p,n}_3]_{J_f}$ stretched configurations are definitely favored in the (^{16}O, ^{12}C) four-nucleon-transfer process. This is due to the fact that the calculated form factor is much more peaked at the nuclear surface for $(2p_{3/2})^4$ configurations than for any $(f_{7/2,5/2})^4$ configurations. It can also be noticed that the $(2p_{1/2})^4_{J=0}$ configuration provides a form factor peaking out much less than the $(2p_{3/2})^4_{J=0}$ configuration. The fact that in ^{44}Ti for the first excited state the $(2p_{3/2})^4_{J_f}$ configuration is present, allowing then strong quartet transfer, has been already pointed out by Arima.[20] This behavior in the case of four-nucleon transfer is of the very same nature as that observed in (t, p) two-neutron transfer for the $(2p_{3/2})^2_{J_f}$ and for the $(1f_{7/2})^2_{J_f}$ configurations in the Ca isotopes.[21]

(3) Analysis of the $^{54}Fe(^{16}O, ^{12}C)^{58}Ni$ angular dis-

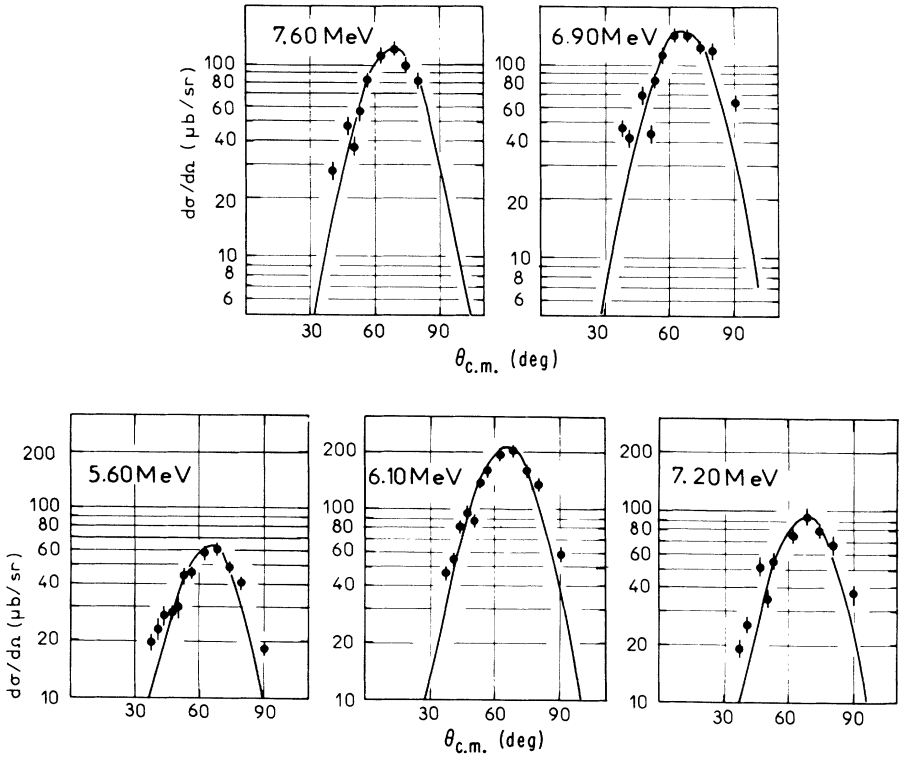

FIG. 5. Experimental $^{54}Fe(^{16}O, ^{12}C)^{58}Ni$ angular distributions measured at ^{16}O 46-MeV incident energy. The curves have been calculated with the Frahn and Venter formulas based on the general diffractional model.

tribution. In Fig. 7 the angular distributions for levels of known spin are presented. They have been successfully fitted in shape with the SETILL code.[19] For the ^{16}O entrance and ^{12}C exit channels we have used the $V_0 = 400$-MeV optical set of Table II, but shape and intensity of the angular distributions are insensitive to any change in possible parameter families in one or both channels, provided V_0 is kept above 100 MeV. It means that the contribution to the T matrix elements is coming only from the nuclear surface. Inside the nucleus, there is a natural cancellation due to the fast oscillatory damping behavior of the optical waves. The wave function of the final states is assumed to be a pure $(2p_{3/2})^4_{J_f}$ stretched wave function. We are assuming then that the ground state, the 1.45-MeV 2^+, and the 3.52-MeV 0^+ states are populated through $(p_{3/2})^4(f_{7/2})^{-2}$ configurations. The ratios $\sigma_{exp}/\sigma_{DWBA}$ are, respectively, 46., 33., and 32., for the ground state, first 2^+ excited state, and the 3.52-MeV 0^+ state. As explained previously the shapes are almost insensitive to any configuration mixing; this is a consequence of dealing with the direct surface reaction.

(4) Q-reaction-value dependence of the cross sections. We now come to the important question of the Q-value dependence. This effect has been estimated in the case of the reaction $^{54}Fe(^{16}O, ^{12}C)^{58}Ni$ for the transition leading to the first 0^+ quartet state at 3.52 MeV. The cross section exhibits strong Q-value dependence as shown in Fig. 8, where we have studied the effect of varying the Q value in the form factor and the optical wave functions of the ^{12}C exit channel:

(i) The dotted line assumes variation only in the form factor (through the four single-particle binding energies);

(ii) in the dot-dashed line, we keep the form factor constant and vary the Q value only in the exit channel;

(iii) the solid line is the realistic case for which both variations are allowed simultaneously according to the relation dictated by energy balance $[Q = |(\text{B.E.})_f(\alpha)| - |(\text{B.E.})_i(\alpha)|]$.

In the latter case, the cross section undergoes a variation of a factor of 2 for a 1-MeV Q-value change, and this effect comes almost exclusively from the mismatch of wave functions in the optical channels as expected from pure semiclassical considerations. The contrast with the light-particle transfers dominated by the form-factor variation is quite clear.

In Ref. 1, the cross sections are given for the first 2^+ excited levels of the various Ti, Cr, Ni, and Zn isotopes reached through (^{16}O, ^{12}C) four-nucleon transfer and measured at 40° lab angle. Thus, for a given series of isotopes, the transfer process occurs through the same dynamical conditions with respect to the Coulomb barrier. As it can be seen from Fig. 9, a strong spectroscopic effect occurs in the region of the zinc isotopes where a ratio of 8.5 is observed for the cross sec-

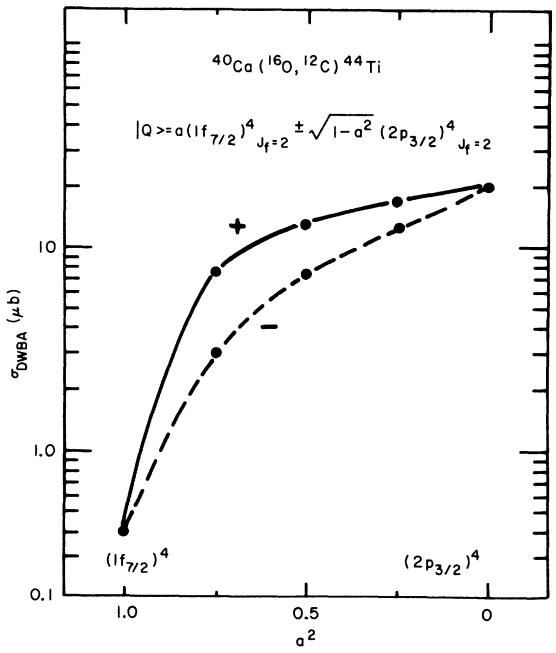

FIG. 6. Variation of the cross-section intensity for different configuration admixtures of the following two stretched components: $(2p_{3/2})^4_{J_f}$ and $(1f_{7/2})^4_{J_f}$.

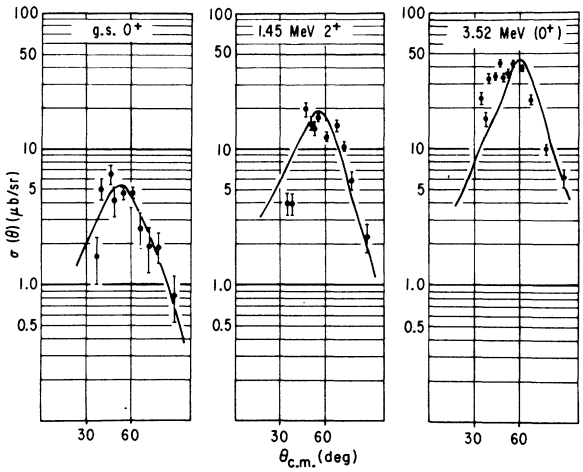

FIG. 7. The angular distribution of the reaction $^{54}Fe(^{16}O, ^{12}C)^{58}Ni$ of the ground state 0^+, the first 2^+ excited state, and the 3.52-MeV 0^+ excited state are fitted in shape using the finite-range DWBA SETILL code. The form factors were calculated assuming that the transfer process populates the stretched configuration $[(2p_{3/2})^{p,n}{}_3(2p_{3/2})^{p,n}{}_3]_{J_f}$.

tions leading to the first 2^+ states in ^{64}Zn and ^{68}Zn for a 1-MeV Q-value difference, whereas purely dynamical mismatch considerations would yield only a factor of 2. The situation is not so obvious for the titanium isotopes, but interesting structure effects appear for Ni and Cr isotopes, where we see that the $^{58}_{28}Ni_{30}$ and $^{60}_{28}Ni_{32}$ cross sections differ by a factor of 2 for only a 1-keV difference in the Q values. Similarly, the ^{52}Cr and ^{54}Cr residual nuclei are reached with a difference in cross sections of a factor of 10 for 880-keV Q-value variations.

The DWBA calculations show clearly, as mentioned before, that the four-nucleon-transfer cross section increases drastically whenever the $(2p_{3/2})^4_{J_f}$ configuration is present. Single-shell-model arguments make this behavior understandable: ^{58}Ni $(2p_{3/2})^4(f_{7/2})^{-2}$ states are easily reached from the $(f_{7/2})^{-2}$ (dominant) component of ^{54}Fe. A target of $^{58}_{26}Fe_{30}$, on the other hand, is well approximated by the $(2p_{3/2})^2(f_{7/2})^{-2}$ configuration, and it is clear that the Pauli exclusion principle will severely decrease the amplitude for formation of $(2p_{3/2})^6(f_{7/2})^{-2}$ states which are the ones favored by the reaction mechanism. Exactly the same kind of arguments apply to the $^{54}_{24}Cr_{30}$ and $^{52}_{24}Cr_{28}$ residual nuclei.

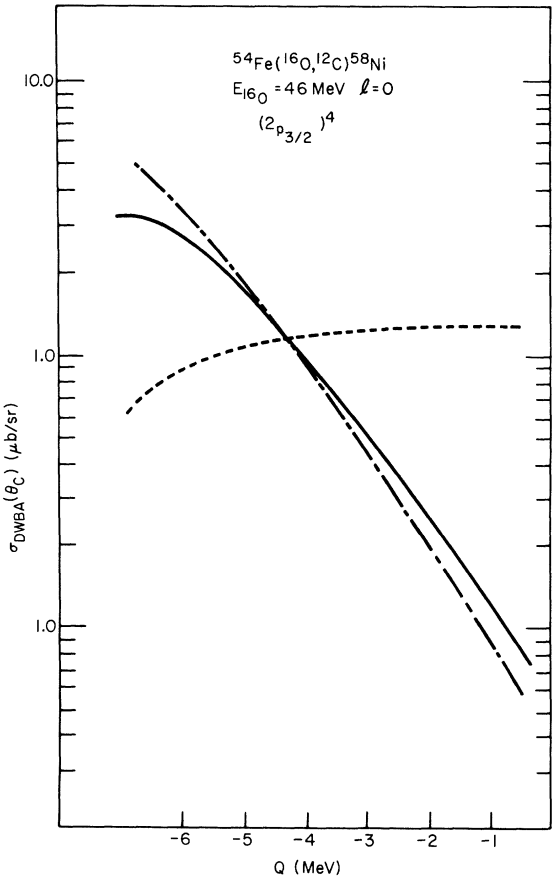

FIG. 8. Q-reaction-value effect. The dotted curve gives the variation of the cross section versus the Q-value changes achieved only in the form-factor calculations [variation of the binding energy $(B.E.)_f(\alpha) = Q + (B.E.)_i(\alpha)$, keeping the Q value constant in the ^{12}C channel]. The dot-dashed curve is the reverse situation: The binding (for Q value) is kept constant in the form factor but is varied in the optical ^{12}C channel. The solid curve corresponds to the realistic case where the Q value is varied both in the form factor and in the optical ^{12}C channel.

VI. CONCLUSION

The purpose of this paper has been threefold: (i) to confirm the possibility of applying the semiclassical approximation of Frahn and Venter to describe the reaction mechanism for heavy-ion four-particle transfers;

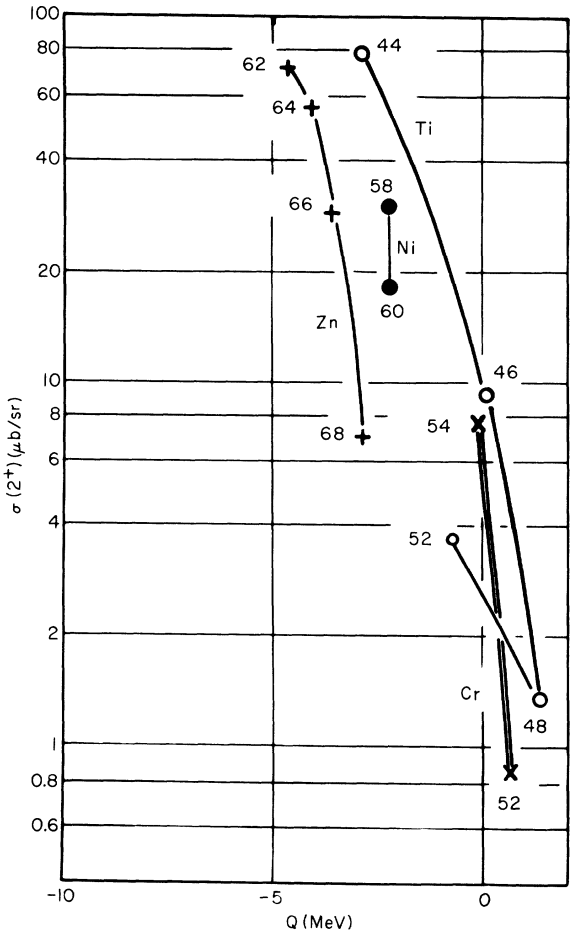

FIG. 9. Cross-section values obtained at 48-MeV ^{16}O incident energy and 40° lab angle of the first 2^+ excited state on various Ti, Cr, Ni, and Zn residual nuclei plotted versus the reaction Q value.

(ii) to test a new method of calculating *DWBA microscopic form factors* which involves a minimum of assumptions beyond the usual one-step-process idea;
(iii) an investigation of the sensitivity of such analysis upon shell-model spectroscopic details.

The (^{16}O, ^{12}C) four-nucleon transfer has been shown to be consistently described by semiclassical considerations even above the Coulomb barrier. The transfer cross sections are peaked at the grazing angle beyond which the Coulomb scattering begins to deviate from the pure Rutherford law. It turns out that the single diffractional model of Frahn and Venter can successfully fit the complete set of four-nucleon-transfer cross sections with only two parameters deduced from the elastic data. It follows that angular distributions provide no clue for spin assignment and that spectroscopic information can be gathered only through the intensity and selectivity of cross sections.

The DWBA calculations performed with the SETILL code have shown the importance of optical-wave-function mismatch in the entrance and exit channels, the Q-value effect in heavy-ion-transfer reactions as expected from simple semiclassical considerations.

The present preliminary DWBA analysis indicates the importance of nuclear-structure effects, in particular the sensitivity of the cross section to the presence of a quartet configuration of the form $[(2p_{3/2})^{p,n}{}_3(2p_{3/2})^{p,n}{}_3]_{J_f}$ in the residual-nucleus wave functions.

We feel that a point has been reached where the possibility of obtaining quantitative information from heavy-ion-transfer data has been shown. A huge spectroscopic effort is now required to establish the spins and parities of the strongly excited peaks so as to allow detailed comparison with nuclear models.

VII. ACKNOWLEDGMENTS

We are very much indebted to A. Pagès and M. Avril for having built most of the essential part of the electronic devices used in the present experiment. Many thanks are due J.-L. Girma and the operating staff of the FN tandem Van de Graaff of Saclay for having provided us a very intense ^{16}O beam on target. It is a pleasure to thank again M. Doury for the preparation of the various targets. We would also like to thank Dr. A. P. Zuker for careful reading of the manuscript.

---

*Visiting scientist on Contract No. BI-II/12766 with the Centre d'Etudes Nucléaires de Saclay and the Centro Siciliano di Fisica Nucleare e Struttura della Materia, Catania. On leave from the Istituto di Fisica Nucleare and the Istituto Nazionale di Fisica Nucleare, Universita di Catania, Italy.

†Permanent address: Laboratoire de Physique Nucléaire, Université de Bordeaux, France.

[1]J.-C. Faivre, H. Faraggi, J. Gastebois, B. G. Harvey, M.-C. Lemaire, J.-M. Loiseaux, M. C. Mermaz, and A. Papineau, Phys. Rev. Letters 24, 1188 (1970); H. Faraggi, A. Jaffrin, M.-C. Lemaire, M. C. Mermaz, J.-C. Faivre, J. Gastebois, B. G. Harvey, J.-M. Loiseaux, and A. Papineau, Ann. Phys. (N.Y.) 66, 905 (1971); H. Faraggi, M.-C. Lemaire, J. M. Loiseaux, M. C. Mermaz, and A. Papineau, Phys. Rev. C 4, 1375 (1971).

[2]V. Gillet, in *Proceedings of the International Conference on Properties of Nuclear States, Montréal, Canada, 1969* (Presses de l'Université de Montréal, Montréal, Canada, 1969), p. 483; J. Phys. (Paris), 32, Colloque C6, C6-17 (1971); A. Arima and V. Gillet, Ann. Phys. (N.Y.), 66, 117 (1971).

[3]W. E. Frahn and R. H. Venter, Nucl. Phys. 59, 651 (1964).

[4]L. C. Northcliffe, Phys. Rev. 120, 1744 (1960); Ann. Rev. Nucl. Sci. 13, 67 (1963).

[5]W. E. Frahn, Phys. Rev. Letters 26, 563 (1971).

[6]W. E. Frahn and R. H. Venter, Ann. Phys. (N.Y.) 24, 243 (1963).

[7]J. S. Blair, Phys. Rev. 95, 1218 (1954).

[8]J. Raynal, Centre d'Etudes Nucléaires, Internal Report No. D.Ph-T/69-42 (unpublished).

[9]G. Igo and R. M. Thaler, Phys. Rev. 106, 126 (1957).

[10]W. Von Oertzen, J. Phys. (Paris) 32, Colloque C6, C6-233 (1971).

[11]P. J. A. Buttle and L. J. B. Goldfarb, Nucl. Phys. A176, 299 (1971).

[12]V. Gillet, B. Giraud, and M. Rho, Nucl. Phys. A103, 57 (1967).

[13]A. Cunsolo, H. Faraggi, M.-C. Lemaire, J.-M. Loiseaux, M. C. Mermaz, A. Papineau, and J.-L. Québert, J. Phys. (Paris) 32, Colloque C6, C6-171 (1971).

[14]P. Beuzit, R. Ballini, J. Delaunay, I. Fodor, J. P. Fouan, and J. Gastebois, J. Phys. (Paris) 32, Colloque C6, C6-139 (1971).

[15]D. F. H. Start, R. Anderson, L. E. Carlson, A. G. Robertson, and M. A. Grace, Nucl. Phys. A162, 49 (1971).

[16]P. Bonche and B. Giraud, in Proceedings of the Second Problem Symposium on Nuclear Physics, Novosibirsk, 1970 (to be published).

[17]B. Giraud, J.-C. Hocquenghem, and A. Lumbroso, Colloque de la Toussuire Report No. LYCEN 71-04, 1971 (unpublished); B. Giraud and D. Zaikine, Phys. Letters 37B, 25 (1971).

[18]J. Griffin and J. Wheller, Phys. Rev. 108, 311 (1957).

[19]P. Bonche, Code SETILL, CEA-Report (to be published).

[20]A. Arima, J. Phys. (Paris) 32, Colloque C6, C6-33 (1971).

[21]R. N. Glover and A. McGregor, Phys. Letters 24B, 97 (1967).